

CUSP SHAPES OF HILBERT-BLUMENTHAL SURFACES AND FLOOR SIMPLICITY

JOSEPH QUINN, ALBERTO VERJOVSKY

INSTITUTO DE MATEMÁTICAS, UNIDAD CUERNAVACA
UNIVERSIDAD NACIONAL AUTÓNOMA DE MÉXICO
AV. UNIVERSIDAD S/N., COL. LOMAS CHAMILPA
C.P. 62210, CUERNAVACA, MORELOS
MÉXICO

josephanthonyquinn@gmail.com

ABSTRACT. We introduce a new fundamental domain \mathcal{R} for a Hilbert modular group Γ over a real quadratic field $K = \mathbb{Q}(\sqrt{n})$ of class number 1, by computing a Dirichlet domain for a cusp section with respect to the classical metric induced by the hyperbolic plane, using lattices in the ring of integers \mathbb{Z}_K . We use \mathcal{R} to plot a cusp section as a 3-dimensional tower that makes explicit its Sol 3-manifold structure and its Anosov diffeomorphism. We also show that the boundary of \mathcal{R} has finite volume when $n = 2, 3, 5$ or 13, whereas previously fundamental domains for Γ with this property had only been known for $n = 5$. For arbitrary n , we show that a finite-volume boundary of M_Γ can always be represented in \mathcal{R} up to affine translations.

1. INTRODUCTION

A Hilbert-Blumenthal group is some $\Gamma = \mathrm{PSL}_2(\mathbb{Z}_K)$ where \mathbb{Z}_K is the ring of integers of a real quadratic field K , and a Hilbert-Blumenthal surface is a quotient $M_\Gamma = (\mathcal{H}^2 \times \mathcal{H}^2)/\Gamma$ of the product of two hyperbolic upper half-planes \mathcal{H}^2 by the Möbius action of Γ under Galois conjugation. As a generalization of modular curves, M_Γ represents the moduli space of Abelian varieties with real multiplication by \mathbb{Z}_K [16] and these complex surfaces are a prototype for Shimura varieties, placing them at an interesting juncture of geometry, topology and number theory.

Here we focus on a fundamental domain R_Γ for the action $\Gamma \curvearrowright \mathcal{H}^2 \times \mathcal{H}^2$ which accurately reflects the geometry of M_Γ , a topic that dates back to Blumenthal's classical publications in *Mathematische Annalen* [2, 3]. Our understanding of R_Γ historically has improved with our understanding of its cusps. Maass [15] showed that the number of cusps equals the class number of K , then Siegel [19] computed an R_Γ as a union over one piece at each cusp using an alternative metric. This yields a complex surface with quotient singularities and cusp singularities, which Hirzebruch [13] showed how to smoothly compactify (see also

Date: May 19, 2022.

[20] and §21 of [1]). While these advances have been fruitful in understanding arithmetic and topological properties of Hilbert modular surfaces, certain geometric properties have remained elusive. Firstly, while it is known that a cusp section of M_Γ is the 3-dimensional mapping torus of some Anosov diffeomorphism φ of the torus, there had previously been no geometric model of this on which φ can be written down in coordinates. Secondly, there had previously been no known R_Γ with a boundary that accurately represents ∂M_Γ as a finite-volume 3-dimensional region. Here we give a new fundamental domain (see Theorem 3.3.4) in the case where M_Γ has one cusp which improves these situations for that setting.

We first construct a fundamental domain $\tilde{\mathcal{R}}$ for the cusp end of M_Γ in which orbit representatives of its maximal unipotent group are minimized with respect to the classical metric on $\mathcal{H}^2 \times \mathcal{H}^2$ induced by the hyperbolic plane (by using a Dirichlet domain for that group). The shape of $\tilde{\mathcal{R}}$ takes an elegant form determined by lattices in the ring of integers \mathbb{Z}_K of K embedded into $\mathcal{H}^2 \times \mathcal{H}^2$ (see Proposition 3.2.3), effectively computable from the fundamental unit ε of \mathbb{Z}_K . From this we form a fundamental domain \mathcal{R} for Γ via intersection with the classical fundamental domain for the inversion map. We give a map $\Psi : \mathcal{H}^2 \times \mathcal{H}^2 \rightarrow \mathbb{R}^3$ with which one can plot the image of a cusp section for each K (see Figure 4), and see the boundary of M_Γ as a continuum of surfaces intersecting the cusp sections as their height lowers (see Figure 5).

By varying K , the cusp sections give the diffeomorphism classes of all Sol 3-manifolds up to commensurability [17, 18]. The current model represents this structure as a multiplication rule on the cusp section under Ψ , as a Lie group. The Anosov diffeomorphism is then multiplication by the fundamental unit ε and its Galois conjugate (see Theorem 4.0.2).

The boundary of a one-cusped Hilbert-Blumenthal surface admits a thick-thin decomposition into a compact region and a cusp end, however the set of orbit representatives in some R_Γ generally fails to approach a finite-volume region. This can be corrected by representing ∂R_Γ up to an equivalence relation on $\mathcal{H}^2 \times \mathcal{H}^2$ via Cohn's [5] notion of the "floor," and a floor is called "simple" when this can be done up to affine translations (see §2.3), but a choice of R_Γ admitting a simple floor had only been known of for the case where $K = \mathbb{Q}(\sqrt{5})$ [12, 5, 7, 10]. The current model \mathcal{R} includes a finite-volume boundary without need for changing representatives, when $n = 2, 3, 5$ or 13 (see Theorem 5.0.1). More generally, the remaining points of M_Γ are always represented up to affine translations over the copies of the cusp sections as their height lowers (see Proposition 5.0.3). This appeals to a looser a sense of Cohn's floor simplicity where we relax a condition due to having a geometrically accurate 3-dimensional model of the cusp section instead of the classical cylinder over a single torus.

2. PRELIMINARIES

2.1. Hilbert-Blumenthal surfaces and cusp sections. Let \mathcal{H}^2 be the upper half-plane model for the hyperbolic plane and denote the usual metric by $d_{\mathcal{H}^2}$. We will be interested in the product space $\mathcal{H}^2 \times \mathcal{H}^2$, in which the points are of the form $(x_1 + y_1 i, x_2 + y_2 i)$ where

$x_1, x_2 \in \mathbb{R}$ and $y_1, y_2 \in \mathbb{R}^+$. We endow $\mathcal{H}^2 \times \mathcal{H}^2$ with the L^1 metric with respect to $d_{\mathcal{H}^2}$,

$$(1) \quad \begin{aligned} d : (\mathcal{H}^2 \times \mathcal{H}^2) \times (\mathcal{H}^2 \times \mathcal{H}^2) &\longrightarrow \mathbb{R}^{\geq 0} \\ ((p_1, p_2), (q_1, q_2)) &\mapsto d_{\mathcal{H}^2}(p_1, q_1) + d_{\mathcal{H}^2}(p_2, q_2). \end{aligned}$$

For $\gamma = \begin{pmatrix} a & b \\ c & d \end{pmatrix} \in \mathrm{PSL}_2(\mathbb{R})$ and $p \in \mathcal{H}^2$, let $\gamma(p)$ denote the usual isometric action by Möbius transformations,

$$\gamma(p) = \frac{ap + b}{cp + d}.$$

Let K be a real quadratic number field and let σ be the non-trivial element of the Galois group $\mathfrak{G}(K : \mathbb{Q})$. That is, $K = \mathbb{Q}(\sqrt{n})$ for some square-free $n \in \mathbb{N}^{>1}$ and $\forall a, b \in \mathbb{Q}$, we have $\sigma(a + b\sqrt{n}) = (a - b\sqrt{n})$. Let \mathbb{Z}_K be the ring of integers of K , i.e. $\mathbb{Z}_K = \mathbb{Z} \oplus \mathbb{Z}\alpha$ where

$$\alpha := \begin{cases} \sqrt{n} & ; \quad n \not\equiv 4 \pmod{4} \\ \frac{1+\sqrt{n}}{2} & ; \quad n \equiv 4 \pmod{4} \end{cases}.$$

Let $\Gamma := \mathrm{PSL}_2(\mathbb{Z}_K)$, then

$$\Gamma \curvearrowright \mathcal{H}^2 \times \mathcal{H}^2 : \quad \gamma(p_1, p_2) = (\gamma(p_1), \sigma(\gamma)(p_2)),$$

is a discrete action by isometries, where $\sigma(\gamma)$ is the result of applying σ to the entries of γ .

Definition 2.1.1.

- (1) We call Γ a Hilbert-Blumenthal group, and we call the orbifold $(\mathcal{H}^2 \times \mathcal{H}^2)/\Gamma$ a Hilbert-Blumenthal surface, which we denote by M_Γ .
- (2) For $p \in \partial(\mathcal{H}^2 \times \mathcal{H}^2)$, the stabilizer of p in Γ , is $\Delta_\Gamma(p) := \{\gamma \in \Gamma \mid \gamma(p) = p\}$.
- (3) The maximal unipotent subgroup (of Γ at p), denoted by $U_\Gamma(p)$, is the group of all unipotent elements of $\Delta_\Gamma(p)$.
- (4) When $U_\Gamma(p) \neq \emptyset$, we say that that Γ (or equivalently that $(\mathcal{H}^2 \times \mathcal{H}^2)/\Gamma$) has a cusp at p , and in this case we call $\Delta_\Gamma(p)$ a cusp group.

Remark 2.1.2. For $\gamma \in \Delta_\Gamma(p)$, the condition that $\gamma \in U_\Gamma(p)$ is equivalent to saying that γ has a unique fixed point as an isometry of $\mathcal{H}^2 \cup \partial\mathcal{H}^2$, which lies in $\partial\mathcal{H}^2$, i.e. that $|\mathrm{tr}(\gamma)| = 2$.

Every cusp group $\Delta_\Gamma(p)$ is conjugate in $\mathrm{PSL}_2(K)$ to $\Delta_\Gamma(\infty, \infty)$. Thus we take $p = (\infty, \infty)$, abbreviate $\Delta := \Delta_\Gamma(p)$ and $U := U_\Gamma(p)$, and this incurs no loss of generality in discussing the cusp shape. As per our discussion of the full group Γ , we assume that there is only one cusp, i.e. that K has class number 1 [15, 20]. Thus, in the following, every cusp group is conjugate in $\mathrm{PSL}_2(\mathbb{Z}_K)$ to Δ . We call $(\mathcal{H}^2 \times \mathcal{H}^2)/\Delta$ the *cusp end* of M_Γ , and denote this by M_Δ .

Matrices in Δ are upper triangular, forcing their diagonal entries to be in the unit group \mathbb{Z}_K^\times . But since K is a real quadratic field, $\mathbb{Z}_K^\times = \{\pm \varepsilon^\ell \mid \ell \in \mathbb{Z}\}$ where ε is the *fundamental unit* of \mathbb{Z}_K , defined by $\varepsilon := \min\{z \in \mathbb{Z}_K^\times \mid z > 1\}$. Thus we have

$$\Delta = \left\{ \begin{pmatrix} \varepsilon^\ell & z \\ 0 & \varepsilon^{-\ell} \end{pmatrix} \mid \ell \in \mathbb{Z}, z \in \mathbb{Z}_K \right\}$$

up to ± 1 , recalling that opposite signs are identified in $\mathrm{PSL}_2(\mathbb{R})$.

Let $\tau_z := \begin{pmatrix} 1 & z \\ 0 & 1 \end{pmatrix}$ where $z \in \mathbb{Z}_K$, then $\forall z \in \mathbb{Z}_K$,

$$(2) \quad \tau_z(x_1 + y_1i, x_2 + y_2i) = \left((x_1 + z) + y_1i, (x_2 + \sigma(z)) + y_2i \right),$$

effecting only the real parts of the points. A computation using the trace shows that $U = \{\tau_z \mid z \in \mathbb{Z}_K\}$, hence $U = \langle \tau_1, \tau_\alpha \rangle$. Let $\eta_\ell := \begin{pmatrix} \varepsilon^\ell & 0 \\ 0 & \varepsilon^{-\ell} \end{pmatrix}$, then

$$(3) \quad \eta_\ell(x_1 + y_1i, x_2 + y_2i) = (\varepsilon^{2\ell}(x_1 + y_1i), \varepsilon^{-2\ell}(x_2 + y_2i)).$$

Let $D := \{\eta_\ell \mid \ell \in \mathbb{Z}\}$, then $D = \langle \eta_1 \rangle$ and $\Delta = \langle \tau_1, \tau_\alpha, \eta_1 \rangle$. The full Hilbert-Blumenthal group is attained by including the element $\iota := \begin{pmatrix} 0 & 1 \\ -1 & 0 \end{pmatrix}$, an inversion through the unit hemisphere in each factor. That is $\Gamma = \langle \tau_1, \tau_\alpha, \eta_1, \iota \rangle$.

The cusp group Δ admits a semi-direct product decomposition, as follows. The group U is a normal subgroup of Δ and since $\mathbb{Z}_K \cong \mathbb{Z} \oplus \mathbb{Z}\alpha$ as an additive group, $U \cong \mathbb{Z}^2$. Also, $D \cong \mathbb{Z}$ is a cyclic subgroup of Δ and U is invariant under conjugation by D , in particular $\eta_\ell \cdot \tau_z \cdot \eta_{-\ell} = \tau_{2\ell z}$. This action by conjugation defines a homomorphism $D \rightarrow \mathrm{Aut}(U)$, giving

$$(4) \quad \Delta \xrightarrow{\cong} U \rtimes D : \quad \begin{pmatrix} \varepsilon^\ell & z \\ 0 & \varepsilon^{-\ell} \end{pmatrix} \mapsto (\tau_z, \eta_\ell).$$

This admits the topological interpretation that M_Δ is diffeomorphic to $T_\varphi^3 \times \mathbb{R}^+$, where T_φ^3 is the infrasolv manifold that fibers over the circle, with fiber the torus [18]. We call T_φ^3 the *cusp section* of M_Γ (or equivalently, of Γ).

2.2. Fundamental domains. A *fundamental domain* for a group G acting on a topological space \mathcal{X} is a subspace of \mathcal{X} , which we will denote by $R_G(\mathcal{X})$ (or just R_G when \mathcal{X} is clear) containing exactly one representative of each orbit of the group action. Some aspects of the classical fundamental domain $R_\Gamma(\mathcal{H}^2 \times \mathcal{H}^2)$ have remained consistent since the classical approach while others have varied. A common theme is the use of an intersection of some choice for R_D , R_U and $R_{\langle \iota \rangle}$, formalized by Götzky [12] and later termed a Götzky region [10].

2.2.1. A fundamental domain for the inversion involution. This aspect has remained the same throughout the literature, dating back to Blumenthal [2], and will be used here as well. Generalizing the fundamental domain $\{p \in \mathcal{H}^2 \mid |p| \geq 1\}$ (where $|\cdot|$ denotes the complex modulus) for the classical modular group $\mathrm{PSL}_2(\mathbb{Z})$ acting on \mathcal{H}^2 , define

$$(5) \quad N : \mathcal{H}^2 \times \mathcal{H}^2 \rightarrow \mathbb{R}^+, \quad (p_1, p_2) \mapsto |p_1||p_2|$$

and let

$$C := \{p \in \mathcal{H}^2 \times \mathcal{H}^2 \mid N(p) \geq 1\}$$

Then $C = R_{\langle \iota \rangle}$.

2.2.2. *A fundamental domain for D.* This aspect also has remained consistent since Blumenthal [2], and will be used here up to a minor alteration. For each $y_1, y_2 \in \mathbb{R}^+$, let

$$(6) \quad \mathcal{F}(y_1, y_2) := \{(x_1 + y_1 i, x_2 + y_2 i) \mid x_1, x_2 \in \mathbb{R}\} \subset \mathcal{H}^2 \times \mathcal{H}^2,$$

the pair of horizontal lines at height y_1 in the first factor and height y_2 in the second factor. Observe that

$$\bigsqcup_{y_1, y_2 \in \mathbb{R}^+} \mathcal{F}(y_1, y_2) = \mathcal{H}^2 \times \mathcal{H}^2,$$

so $\mathcal{F} := \{\mathcal{F}(y_1, y_2)\}_{y_1, y_2 \in \mathbb{R}^+}$ foliates $\mathcal{H}^2 \times \mathcal{H}^2$. There is a natural bijection

$$(7) \quad \Pi : \mathcal{F} \rightarrow \mathbb{R}^+ \times \mathbb{R}^+, \quad \mathcal{F}(y_1, y_2) \mapsto (y_1, y_2).$$

By equation (3), D permutes the leaves via

$$(8) \quad \eta_\ell(\mathcal{F}(y_1, y_2)) = \mathcal{F}(\varepsilon^{2\ell} y_1, \varepsilon^{-2\ell} y_2),$$

thus in the image under Π , D preserves each hyperbola in the set $\{y_1 y_2 = c \mid y_1, y_2 \in \mathbb{R}^+\}_{c \in \mathbb{R}^+}$, which foliates $\mathcal{H}^2 \times \mathcal{H}^2$ under Π^{-1} .

A natural fundamental domain for the action of D is thus obtained as Π^{-1} of the wedge between a pair of rays approaching the origin, identified by η_1 . Our choice of these rays will be justified in §3.3, and we define our fundamental domain for D as

$$R_D := \Pi^{-1} \left(\{(y_1, y_2) \in \mathbb{R}^+ \times \mathbb{R}^+ \mid y_2 \leq y_1 < \varepsilon^4 y_2\} \right).$$

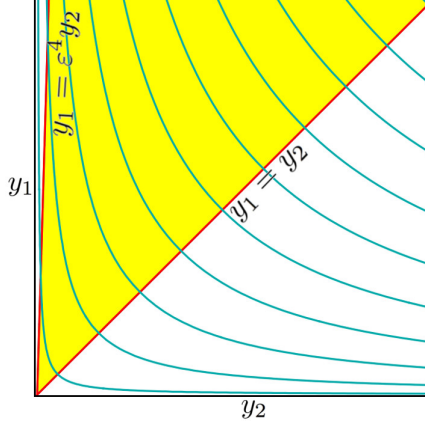


FIGURE 1. [14] The fundamental domain R_D is shown (in yellow) for the action of D on \mathcal{F} , along with a D-invariant foliation by hyperbolas (in cyan).

2.2.3. Fundamental domains for U . By equation (2), U fixes each leaf of the foliation \mathcal{F} , and since $\Delta = D \rtimes U$, we have that $R_U \cap R_D$ is a fundamental domain for Δ regardless of one's choice of R_U . Topologically, each quotient $\mathcal{F}(y_1, y_2)/U$ is a flat torus and \mathcal{F}/U is foliated by these tori. If one is interested in arithmetic properties of M_Γ as a topological manifold, one can represent orbits of U as Siegel [19] does, using a reduction with respect to the field norm on K .

Seeking a geometric representation of M_Γ , our approach aligns better with that of Cohn [6, 5, 7, 8], but with an important distinction which we will explain after discussing the parts in common. Define the *height* of a leaf $\mathcal{F}(y_1, y_2)$ in the foliation \mathcal{F} , or of a point $(x_1 + y_1i, x_2 + y_2i)$ in the leaf, as the product y_1y_2 . A set of points at some fixed height corresponds to Π^{-1} of a hyperbola in Figure 1. A set of points at Π^{-1} of the piece of a hyperbola between the rays $y_1 = y_2$ and $y_1 = \varepsilon^4 y_2$ gives a homeomorphic representation of the cusp section, and the points at Π^{-1} of the entire wedge between these rays gives a homeomorphic representation of the cusp end M_Δ .

We differ from Cohn's approach in the following way. Cohn chooses R_U to be the set of points $(x_1 + y_1i, x_2 + y_2i) \in \mathcal{H}^2 \times \mathcal{H}^2$ where $x_1 = r_1 + r_2\alpha$ and $x_2 = r_1 + r_2\bar{\alpha}$ with $-\frac{1}{2} \leq r_\ell < \frac{1}{2}$ ($\ell = 1, 2$). While this gives a straightforward fundamental domain for Δ in analogy to the classical cusp group of $\mathrm{PSL}_2(\mathbb{Z})$, it does not account for the change in metric that occurs in the leaves as the level varies. We will choose R_U differently. Define the *level* of a ray as in Figure 1, or of a point $(x_1 + y_1i, x_2 + y_2i)$ in a leaf on this ray, as the quotient $\frac{y_1}{y_2}$. There is a natural bijection at each leaf

$$(9) \quad \pi_{y_1, y_2} : \mathcal{F}(y_1, y_2) \rightarrow \mathbb{R}^2, \quad (x_1 + y_1i, x_2 + y_2i) \mapsto (x_1, x_2).$$

Under these bijections, points at the same level (varying the height) correspond to spaces where the metric d (see (1)) scales uniformly, and points at the same height (varying the level) correspond to spaces where d expands along one axis and contracts along another. We will represent (in §3.2) the orbit of U by tori that change shape as the leaves vary, to capture this change in geometry.

2.3. Floors. Cohn [5] introduced the notion of a floor as a way of controlling geometrically awkward behavior at the boundary of R_Γ . In particular, a fundamental domain R_Δ in general fails to provide a fundamental domain $R_\Gamma = R_\Delta \cap C$ for Γ with a finite-volume boundary, so the idea is to find an alternative way to represent ∂M_Γ inside of R_Γ .

A point $p = (x_1 + y_1i, x_2 + y_2i) \in R_\Gamma$ is said to *lie over* a point $p' = (x_1 + y'_1i, x_2 + y'_2i)$ when $\frac{y_1}{y_2} = \frac{y'_1}{y'_2}$ but $y_1y_2 > y'_1y'_2$, i.e. the points have the same real coordinates and the same level, but the height of p is greater than the height of p' . When every point in $R_\Gamma \setminus \partial R_\Gamma$ lies over some point in ∂C , we have that $\partial R_\Gamma \subset \partial C$, and ∂R_Γ has finite volume. When this is not the case, one looks for this to happen up to translations, i.e. that $\forall p \in R_\Gamma, \exists \tau \in U$ such that $\tau(p)$ lies over ∂C , but this incurs the possibility of identifying ∂R_Γ with ∂C in several disconnected pieces, resulting from the use of different translations at different levels. Computationally, specifying these pieces is highly nontrivial [7, 10], and Cohn shows that there is a single one of these pieces only when $n = 5$ [5].

When $n = 2, 3, 5$ or 13 , the boundaries of the fundamental domains we introduce are contained in ∂C as one piece homeomorphic to the cusp section, without need for changing any orbit representatives. In dealing with the cases where this fails, we point out that Cohn's definition of floor simplicity had only been applied to Götzky regions where R_U is as described in the last paragraph of §2.2.3, and that the definition of a floor may have been complicated by the need to find the boundary using a single torus. Since the motivation is to visualize ∂M_Γ as a single piece, we will choose the following (weaker) definition of simplicity, which suffices in our model for giving a homeomorphic image of ∂M_Γ up to translations.

Definition 2.3.1. *R_Γ has an affine-simple floor when $\forall p \in \partial R_\Gamma, \exists \tau \in U$ such that $\tau(p)$ lies over ∂C .*

2.4. Dirichlet domains. When \mathcal{X} is a metric space, we can use its metric to form a type of fundamental domain with additional geometric properties.

Definition 2.4.1. *If G is a group of isometries acting on a metric space \mathcal{X} with metric $d_{\mathcal{X}}$, and $c \in \mathcal{X}$ is a point such that $\Delta_G(c) = \{1\}$, then the Dirichlet domain for G centered at c is*

$$\mathcal{D}_c(G) := \left\{ x \in \mathcal{X} \mid \forall \gamma \in \Gamma, d_{\mathcal{X}}(c, x) \leq d_{\mathcal{X}}(c, \gamma(x)) \right\}.$$

Then $\mathcal{D}_c(G)$ is convex and tiles \mathcal{X} under the group action. Each pair of sides of $\mathcal{D}_c(G)$ is contributed by an isometry and its inverse, which are identified by that isometry under the group action. The set of isometries that contribute the sides of $\mathcal{D}_c(G)$ generate the group G . [11] We can identify $\mathcal{D}_c(G)$ and its sides with the following tools.

Definition 2.4.2. *Let \mathcal{X} be a geometry with distance function $d_{\mathcal{X}}$.*

(1) *The mediatrix between p and q is*

$$m_{p,q} := \{x \in \mathcal{X} \mid d_{\mathcal{X}}(p, x) = d_{\mathcal{X}}(q, x)\}.$$

(2) *For an isometry $g \in \text{Isom}^+(\mathcal{X})$ and a point $c \in \mathcal{X}$ at which $g(c) \neq c$, the mediatrix contributed by g is $m_c(g) := m_{c,g(c)}$, or just $m(g)$ when c is clear.*

(3) *The the semi-space contributed by g is*

$$E_c(g) := \{x \in \mathcal{X} \mid d_{\mathcal{X}}(p, x) \leq d_{\mathcal{X}}(q, x)\},$$

or just $E(g)$ when c is clear.

Remark 2.4.3. *We prefer the Spanish term “mediatrix” (plural is “mediatrices”) to the more common term “perpendicular bisector” because the latter suggests that there is a unique geodesic between any two points (to be perpendicularly bisected). This is not true in $\mathcal{H}^2 \times \mathcal{H}^2$ since its metric is the L_1 sum over the \mathcal{H}^2 metrics, similarly to how the Manhattan metric does not give unique geodesics.*

It follows that Definition 2.4.1 is equivalent to

$$\mathcal{D}_c(G) = \bigcap_{g \in G \setminus \{1\}} E_c(g).$$

3. FUNDAMENTAL DOMAINS FOR U , Δ AND Γ

In this section, we construct a Dirichlet domain $\mathcal{D}_c(U)$, then intersect it with R_D and $R_D \cap C$ to attain a fundamental domains for Δ and Γ , respectively. Since the sides of a Dirichlet domain are portions of mediatrixes, we begin with a characterization of these.

3.1. Mediatrixes in $\mathcal{H}^2 \times \mathcal{H}^2$. We will simplify the computation of mediatrixes using the function

$$(10) \quad \delta_1 : \mathcal{H}^2 \times \mathcal{H}^2 \rightarrow \mathbb{R}^+, \quad (p, q) \mapsto \frac{|p - q|^2}{\Im(p)\Im(q)}.$$

While δ_1 is not a distance function (it fails to satisfy the triangle inequality), it does satisfy the following properties.

Lemma 3.1.1.

- (1) *The function δ_1 is invariant under the action of $\mathrm{PSL}_2(\mathbb{R})$.*
- (2) *For all $p, q \in \mathcal{H}^2$, $m_{p,q} = \{x \in \mathcal{H}^2 \mid \delta_1(p, x) = \delta_1(q, x)\}$.*
- (3) *Whenever $d_{\mathcal{H}^2}(p, q) > d_{\mathcal{H}^2}(p, q')$, we have $\delta_1(p, q) > \delta_1(p, q')$.*

Proof. The distance formula on \mathcal{H}^2 is

$$d_{\mathcal{H}^2}(p, q) = \log \left(x + \sqrt{x^2 - 1} \right)$$

where

$$x = 1 + \frac{\delta_1(p, q)}{2}.$$

Therefore $\delta_1(p, q)$ constitutes the part of $d_{\mathcal{H}^2}(p, q)$ that depends on p and q , so since $d_{\mathcal{H}^2}$ is invariant under the action of $\mathrm{PSL}_2(\mathbb{R})$, so is δ_1 .

Specifically, the strictly increasing bijection

$$F : \mathbb{R}^{\geq 0} \rightarrow \mathbb{R}^{\geq 0}, \quad t \mapsto e^r + e^{-r} - 2$$

satisfies $F \circ d_{\mathcal{H}^2} = \delta_1$. Thus for any fixed pair of points $p, q \in \mathcal{H}^2$, the set of points $x \in \mathcal{H}^2$ satisfying the inequality

$$d_{\mathcal{H}^2}(p, x) \leq d_{\mathcal{H}^2}(q, x)$$

is the same as those satisfying the inequality

$$\delta_1(p, x) \leq \delta_1(q, x).$$

□

Extend δ_1 to the function

$$(11) \quad \begin{aligned} \delta : (\mathcal{H}^2 \times \mathcal{H}^2) \times (\mathcal{H}^2 \times \mathcal{H}^2) &\rightarrow \mathbb{R}^+, \\ ((p_1, p_2), (q_1, q_2)) &\mapsto \delta_1(p_1, q_1) + \delta_1(p_2, q_2) = \frac{|p_1 - q_1|^2}{\Im(p_1)\Im(q_1)} + \frac{|p_2 - q_2|^2}{\Im(p_2)\Im(q_2)}. \end{aligned}$$

It follows from Lemma 3.1.1 that this is invariant under $\mathrm{PSL}_2(\mathbb{R}) \times \mathrm{PSL}_2(\mathbb{R})$, and that

$$m_{p,q} = \{x \in \mathcal{H}^2 \mid \delta(p, x) = \delta(q, x)\}.$$

As before, denote a point in $\mathcal{H}^2 \times \mathcal{H}^2$ by $(x_1 + y_1 i, x_2 + y_2 i)$ where $x_1, x_2 \in \mathbb{R}$ and $y_1, y_2 \in \mathbb{R}^+$, and recall that $\tau_z = \begin{pmatrix} 1 & z \\ 0 & 1 \end{pmatrix}$ where $z \in \mathbb{Z}_K$. Let $c' \in \mathbb{R}^+$, let $c = (c'i, c'i) \in \mathcal{H}^2 \times \mathcal{H}^2$ and abbreviate $m(\tau_z) = m_c(\tau_z)$ and $E(\gamma) = E_c(\gamma)$.

Lemma 3.1.2. *The semi-space $E(\tau_z)$ is the solution set to*

$$\frac{2x_1z - z^2}{y_1} + \frac{2x_2\sigma(z) - \sigma(z)^2}{y_2} \leq 0$$

and the mediatrix $m(\tau_z)$ is the set of points at equality.

Proof. Via Lemma 3.1.1, we use δ to compute that the semi-space $E(\gamma)$ is the set of points satisfying the inequality

$$\frac{x_1^2 + y_1^2 + c'^2 - 2c'y_1}{c'y_1} + \frac{x_2^2 + y_2^2 + c'^2 - 2c'y_2}{c'y_2} \leq \frac{|x_1 + y_1 i - \gamma(c'i)|^2}{\Im(\gamma(c'i)) y_1} + \frac{|x_2 + y_2 i - \sigma(\gamma)(c'i)|^2}{\Im(\sigma(\gamma)(c'i)) y_2}$$

and that the mediatrix $m(\gamma)$ is the set of points at equality. Letting σ be the nontrivial element of the Galois group $\mathfrak{G}(K : \mathbb{Q})$, we have

$$\tau_z((c'i, c'i)) = (c'i + z, c'i + \sigma(z)).$$

Substituting this into the previous display gives the desired formula. \square

Remark 3.1.3. *We can similarly derive formulas for mediatrices contributed by other elements of Δ but the formulas are more complicated. These do admit a nice characterization as projections to pairs of arcs (or rays in the case of U) approaching pairs of points on each $\partial\mathcal{H}^2$ factor, but nonetheless the sides of a Dirichlet domain $\mathcal{D}(\Gamma)$ (or even $\mathcal{D}(\Delta)$) are difficult to control. Thus we prefer to use the classical fundamental domains for D and $\langle i \rangle$.*

3.2. A Dirichlet domain for U . Recall that each leaf $\mathcal{F}(y_1, y_2)$ (as defined by equation (2)) is invariant under the action of U . Thus the Dirichlet domain $\mathcal{D}_c(U)$ in $\mathcal{H}^2 \times \mathcal{H}^2$ can be realized as a union over $y_1, y_2 \in \mathbb{R}^+$ of slices

$$(12) \quad T(y_1, y_2) := \mathcal{D}_c(U) \cap \mathcal{F}(y_1, y_2).$$

We have $\pi_{y_1, y_1}(c) = (0, 0)$, and the orbit of $(0, 0)$ under U in this projection is the same for all y_1, y_2 , but the portion of a mediatrix that intersects $\mathcal{F}(y_1, y_2)$ varies due to the change in the metric. The first thing we want to control is the shape of the regions $T(y_1, y_2)$.

Lemma 3.2.1.

- (1) *If $\frac{y_1}{y_2} = \frac{y'_1}{y'_2}$, then $\pi_{y_1, y_2}(T(y_1, y_2)) = \pi_{y'_1, y'_2}(T(y'_1, y'_2))$.*
- (2) *For each $y_1, y_2 \in \mathbb{R}^+$, $\pi_{y_1, y_2}(T(y_1, y_2))$ is either a parallelogram or hexagon symmetric about $(0, 0)$, and varies continuously with y_1, y_2 .*

Proof. The mediatrix for τ_z acting on $\mathcal{F}(y_1, y_2)$ for some fixed $y_1, y_2 \in \mathbb{R}^+$ is $m(\tau_z) \cap \mathcal{F}(y_1, y_2)$. By Lemma 3.1.2, this is the solution set to

$$(13) \quad 2x_1z - z^2 + \frac{y_1}{y_2} (2x_2\sigma(z) - \sigma(z)^2) = 0$$

in the (x_1, x_2) -coordinates. Part (1) follows immediately. Also, each such mediatrix is a Euclidean line and changes continuously with the choice of $y_1, y_2 \in \mathbb{R}^+$.

Since $\{(z, \sigma(z)) \mid z \in \mathbb{Z}_K\} \subset \mathbb{R}^2$ is discrete, there are finitely many lines $m(z) \cap \mathcal{F}(y_1, y_2)$ contributing sides to $\pi_{y_1, y_2}(\mathcal{T}(y_1, y_2))$. Also, since $\forall z \in \mathbb{Z}_K$, $-z \in \mathbb{Z}_K$ and $\sigma(-z) = -\sigma(z)$, these lines are arranged symmetrically about the origin. Since $\mathcal{T}(y_1, y_2)$ is a Dirichlet domain for the action of U on $\mathcal{F}(y_1, y_2)$, it is convex and tiles the plane via translational symmetry. The only possible number of sides for a convex Euclidean polygon that does this are 3, 4 and 6, but since $\mathcal{T}(y_1, y_2)$ has order 2 rotational symmetry, the number of sides must be 4 or 6. \square

Remark 3.2.2. *This deforms the representation of the orbits of U as the leaf varies. Each side of a torus is a segment of a mediatrix $m(\tau_z)$, and thus the orbits are given in the generators z contributing these mediatrix, for instance the way one would use 1 and \sqrt{d} (when $d \not\equiv 4 \pmod{4}$) in the Euclidean cross-sections.*

Assembling these gives

$$\mathcal{D}_c(U) = \bigsqcup_{y_1, y_2 \in \mathbb{R}^+} \mathcal{T}(y_1, y_2).$$

Moreover, we can control the distribution of the parallelograms in $\mathcal{D}_c(U)$ and which $z \in \mathbb{Z}_K$ contribute them, as follows.

Proposition 3.2.3. *The parallelogram cross-sections of $\mathcal{D}_c(U)$ are distributed discretely along the axis of symmetry in the following way. If $\mathcal{T}(y_1, y_2)$ is a parallelogram whose sides are contributed by $\pm z, \pm z' \in \mathbb{Z}_K$, then $\frac{y_1}{y_2} = \frac{-zz'}{\sigma(zz')}$. The next parallelogram as $\frac{y_1}{y_2}$ increases is contributed by $\pm(z+z')$ and whichever of the pairs $\pm z$ or $\pm z'$ that has smaller absolute value under σ .*

Proof. By Lemma 3.2.1, it suffices to look at $\mathcal{T}(h, 1)$ where $h = \frac{y_1}{y_2}$ (the height). For $z \in \mathbb{Z}_K$ denote the line $\pi_{h,1}(m(\tau_z) \cap \mathcal{F}(h, 1))$ by l_z . Now fix $z, z' \in \mathbb{Z}_K^+$ with $z \neq z'$, and let P be the parallelogram bounded by $l_{\pm z}$ and $l_{\pm z'}$. Using equation (13), we compute that $l_{\pm z} \cap l_{\pm z'} \cap l_{\pm(z+z')}$ and $l_{\pm z} \cap l_{\mp z'} \cap l_{\pm(z-z')}$ are two pairs of corners of P when $h = -\frac{zz'}{\sigma(zz')}$, otherwise are empty.

Moreover, increasing h slightly changes the slopes of the lines so that the point $l_z \cap l_{z'} \cap l_{z+z'}$ expands to a line segment connecting $l_z \cap l_{z+z'}$ to $l_{z'} \cap l_{z+z'}$ inside of P , and the point $l_z \cap l_{-z'} \cap l_{z-z'}$ expands to a line segment connecting $l_z \cap l_{z-z'}$ to $l_{-z} \cap l_{z-z'}$ outside of P . Decreasing h slightly has the opposite effect. Thus the 8 lines $l_{\pm z}, l_{\pm z'}, l_{\pm(z+z')}$ and $l_{\pm(z-z')}$ bound a parallelogram when $h = -\frac{zz'}{\sigma(zz')}$ and otherwise bound a hexagon. This suffices to show that whenever $\mathcal{T}(h, 1)$ is a parallelogram, h is as stated. The discreteness of $\{(z, \sigma(z)) \mid z \in \mathbb{Z}_K\}$ gives that the parallelograms are discretely distributed.

Lastly, increasing h deforms P so that the pair of edges contributed by $l_{\pm(z+z')}$ expands. Thus the next time that the cross section is a parallelogram, it will be bounded by two pairs of opposite edges from among the sides of an intermediary hexagon, necessarily including

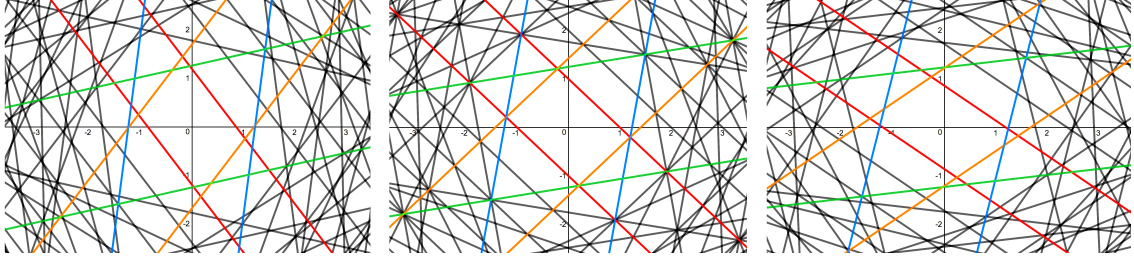


FIGURE 2. [4] Some lines $\{m(\tau_z) \cap \mathcal{F}(h, 1) \mid z \in \mathbb{Z}_K\}$ in the case $n = 2$ exemplify the situation described in the proof of Proposition 3.2.3. The lines at $\frac{y_1}{y_2} = 1$ are in the center, and those with $\frac{y_1}{y_2}$ slightly decreased and increased are shown on the left and right, respectively. The pairs of lines for $z = \pm 1, \pm \sqrt{n}, \pm(1 + \sqrt{n})$ and $\pm(1 - \sqrt{n})$ are colored red, orange, blue and green, respectively, and the lines for all other $z \in \mathbb{Z}_K$ that enter the shown region are shown in black.

the pair contributed by $\pm(z + z')$. Again analyzing the slope of the lines under this deformation, we see that $l_{\pm z}$ move outside of P if and only if $|\sigma(z)| < |\sigma(z')|$, so the one with lower absolute value under σ persists in contributing a boundary as the other vanishes. \square

There is more detail in Proposition 3.2.3 than is used in the theorems, which is indispensable in computing examples (e.g. in Figure 4 and Table 1).

3.3. A Fundamental Domain for Δ . The Dirichlet domain $\mathcal{D}_c(U)$ easily gives rise to a fundamental domain for Δ via intersection with R_D (from §2.2). To obtain a precise description of this, we establish some properties at the boundaries of the intersection.

While it is nontrivial to compute the sides $T(y_1, y_2)$ given only y_1, y_2 and n , we can do this at some key locations. First, we take advantage of the fact that the metric on $\mathcal{F}(y_1, y_2)$ is Euclidean when $y_1 = y_2$, justifying our choice of this as a boundary line for R_D under Π (as in Figure 1).

Lemma 3.3.1.

(1) *If $n \not\equiv_4 1$, then $T(y, y)$ is a rectangle whose sides are contributed by the $m(\tau_z)$ where*

$$z \in \{\pm 1, \pm \sqrt{n}\}.$$

(2) *If $n \equiv_4 1$, then $T(y, y)$ is a hexagon whose sides are contributed by the $m(\tau_z)$ where*

$$z \in \left\{ \pm 1, \pm \frac{1 + \sqrt{n}}{2}, \pm \frac{1 - \sqrt{n}}{2} \right\}.$$

Proof. By Lemma 3.2.1, it suffices to consider $y = 1$.

For an element $z = a + b\sqrt{n} \in \mathbb{Z}_K$ with $a, b \in \mathbb{Q}$, we have

$$(\pi_{1,1} \circ \tau_z|_{\mathcal{F}(1,1)})(c) = (a + b\sqrt{n}, a - b\sqrt{n}).$$

Therefore the orbit of U on c at $\mathcal{F}(1, 1)$ forms a rectangular lattice if $n \not\equiv 4 \pmod{4}$, and forms a triangular lattice if $n \equiv 4 \pmod{4}$, where in both cases the lattice has the diagonal lines of symmetry $x_1 = \pm x_2$. Also, taking $y_1 = y_2$ in equation (13), the mediatrixes $m(\tau_z) \cap \mathcal{F}(1, 1)$ are the Euclidean perpendicular bisectors between the points $(0, 0)$ and $(z, \sigma(z))$. Thus $T(1, 1)$ is rectangular if $n \not\equiv 4 \pmod{4}$ and hexagonal if $n \equiv 4 \pmod{4}$ (see Figure 3).

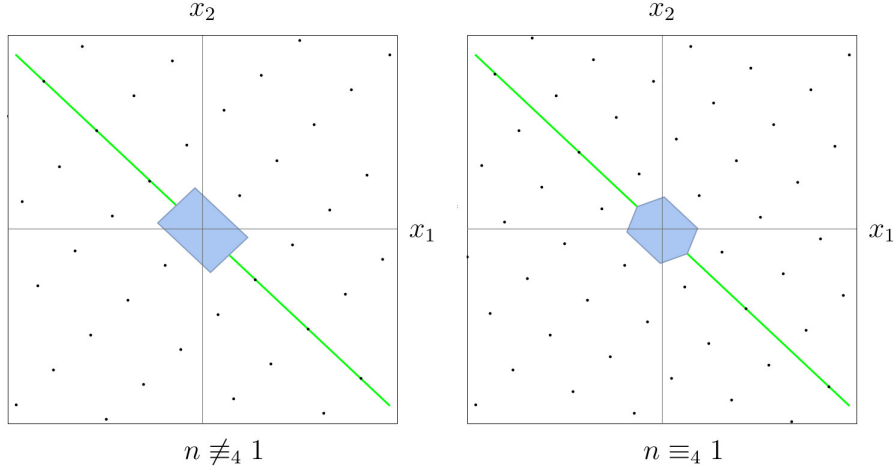


FIGURE 3. [14] The points show the lattice formed by the orbit of U on $(0, 0)$ in $\pi_{y,y}(\mathcal{F}(y, y))$, with the line of symmetry $x_1 = -x_2$ shown in green. In this case the Dirichlet domain $T(y, y)$ for U in $\mathcal{F}(y, y)$ is the Euclidean one, shown in blue.

In both cases, sides are contributed by the orbit points closest to the origin, which are $(\pi_{1,1} \circ \tau_{\pm 1}|_{\mathcal{F}(1,1)})(c) = \pm(1, 1)$. Additional sides are then contributed by the closest points to the origin that lie between the lines

$$\pi_{1,1}(m(\tau_{\pm 1}) \cap \mathcal{F}(1, 1)) = \{(x_1, x_2) \mid x_1 + x_2 = \pm 1\}.$$

When $n \not\equiv 4 \pmod{4}$, these are $\pm\left(\frac{\sqrt{n}}{2}, -\frac{\sqrt{n}}{2}\right)$ (from taking $z = \pm\sqrt{n}$) and when $n \equiv 4 \pmod{4}$, they are $\pm\left(\frac{1+\sqrt{n}}{2}, \frac{1-\sqrt{n}}{2}\right)$ and $\pm\left(\frac{1-\sqrt{n}}{2}, \frac{1+\sqrt{n}}{2}\right)$ (from taking $z = \pm\frac{1+\sqrt{n}}{2}$ and $\pm\frac{1-\sqrt{n}}{2}$, respectively). \square

Next we characterize the sides of the tori associated (under Π) to the points along the ray where $y_1 = \varepsilon^4 y_2$, the other boundary of $\mathcal{D}_c(U) \cap R_D$ (as in Figure 1). These are the tori $\{T(\varepsilon^2 s, \varepsilon^{-2} s) \mid s \in \mathbb{R}^+\}$ and, as the next lemma shows, listing their sides is just a matter of knowing the fundamental unit ε .

This can be done in terms of the elements $z \in \mathbb{Z}_K$ such that $\tau_z \in U$ contributes a side (in which case we will abbreviate our terminology by saying that z *contributes a side*), or it can be done in terms of the (x_1, x_2) -coordinates under the maps $\{\pi_{\varepsilon^2 s, \varepsilon^{-2} s}\}_{s \in \mathbb{R}^+}$. For the

latter characterization we define, for $z \in \mathbb{Z}_K$, the map

$$(14) \quad z *_{\sigma} : \mathcal{H}^2 \times \mathcal{H}^2 \rightarrow \mathcal{H}^2 \times \mathcal{H}^2, \quad (x_1 + y_1 i, x_2 + y_2 i) \mapsto (zx_1 + y_1 i, \sigma(z)x_2 + y_2 i).$$

Lemma 3.3.2. *The polygon $T(\varepsilon^2 y, \varepsilon^{-2} y)$ has the same number of sides as $T(y, y)$ and these are contributed by the isometries εz over the z values indicated in Lemma 3.3.1. Moreover, $\varepsilon *_{\sigma} (T(\varepsilon^2 y, \varepsilon^{-2} y)) = \eta_1(T(y, y))$.*

Proof. Again by Lemma 3.2.1, it suffices to consider $y = 1$. We will do the case where $n \not\equiv 4 \pmod{4}$, and we point out that a similar (but longer) computation applies in the other case.

By Lemma 3.3.1 and equation (13),

$$T(1, 1) = \{(x_1, x_2) \in \mathcal{F}(1, 1) \mid |x_1 + x_2| < 1, |x_1 - x_2| < \sqrt{n}\},$$

thus no mediatrix enters this region. Solving for x_2 in terms of x_1 in the equation (13) for an arbitrary mediatrix in $\mathcal{F}(y, y)$, and substituting this into the defining inequalities of the set above, this is equivalent to saying that there is no choice of $z \in \mathbb{Z}_K$ and $x_1 \in \mathbb{R}$ that simultaneously satisfies the two inequalities

$$(15) \quad \begin{aligned} \left| \left(1 - \frac{z}{\sigma(z)}\right) x_1 + \frac{z^2 + \sigma(z)^2}{2\sigma(z)} \right| &> 1, \\ \left| \left(-1 - \frac{z}{\sigma(z)}\right) x_1 + \frac{z^2 + \sigma(z)^2}{2\sigma(z)} \right| &> \sqrt{n}. \end{aligned}$$

We will use this to get a contradiction.

For the next step, it matters whether $\sigma(\varepsilon) = \varepsilon^{-1}$ or $-\varepsilon^{-1}$, but the arguments are the same up to a sign change, so we assume without loss of generality that $\sigma(\varepsilon) = \varepsilon^{-1}$. Let

$$P = \{m(\tau_z) \cap \mathcal{F}(\varepsilon^2, \varepsilon^{-2}) \mid z = \pm\varepsilon, \pm\varepsilon\sqrt{n}\}.$$

Via equation (13), $\pi_{\varepsilon^2, \varepsilon^{-2}}(m(\tau_z) \cap \mathcal{F}(\varepsilon^2, \varepsilon^{-2}))$ is the Euclidean line in the coordinates $(x_1, x_2) \in \mathbb{R}^2$ with equation

$$(16) \quad zx_1 + \varepsilon^4 \sigma(z) x_2 - \frac{z^2 + \varepsilon^4 \sigma(z)^2}{2} = 0,$$

thus

$$P = \{(x_1, x_2) \in \mathcal{F}(\varepsilon^2, \varepsilon^{-2}) \mid |x_1 + \varepsilon^2 x_2| < \varepsilon, |x_1 - \varepsilon^2 x_2| < \varepsilon\sqrt{n}\}.$$

Writing x_2 in terms of x_1 in equation (16), the portion of an arbitrary mediatrix entering P would have to simultaneously satisfy the two inequalities

$$\begin{aligned} \left| \left(1 - \varepsilon^{-2} \frac{z}{\sigma(z)}\right) x_1 + \frac{\varepsilon^{-2} z^2 + \varepsilon^2 \sigma(z)^2}{2\sigma(z)} \right| &> \varepsilon, \\ \left| \left(1 + \varepsilon^{-2} \frac{z}{\sigma(z)}\right) x_1 - \frac{\varepsilon^{-2} z^2 + \varepsilon^2 \sigma(z)^2}{2\sigma(z)} \right| &> \varepsilon\sqrt{n}. \end{aligned}$$

But making the change of variables $z = \varepsilon z' \in \mathbb{Z}_K$ and $x_1 = \varepsilon x'_1 \in \mathbb{R}$, these are equivalent to inequalities (15), a contradiction. Thus no mediatrixes enter P , hence P is the boundary of $T(\varepsilon^2, \varepsilon^{-2})$.

For the “moreover” part, using equation (13) again, we compute that the corners of $\pi_{1,1}(\eta_1(T(1,1)))$ are

$$\pm \left(\varepsilon^2 \frac{1+\sqrt{n}}{2}, \varepsilon^{-2} \frac{1-\sqrt{n}}{2} \right), \pm \left(\varepsilon^2 \frac{1-\sqrt{n}}{2}, \varepsilon^{-2} \frac{1+\sqrt{n}}{2} \right),$$

and that the corners of $\pi_{\varepsilon^2, \varepsilon^{-2}} T(\varepsilon^2, \varepsilon^{-2})$ are

$$\pm \left(\varepsilon \frac{1+\sqrt{n}}{2}, \sigma(\varepsilon) \frac{1-\sqrt{n}}{2} \right), \pm \left(\varepsilon \frac{1-\sqrt{n}}{2}, \sigma(\varepsilon) \frac{1+\sqrt{n}}{2} \right),$$

and since $\varepsilon^2 = \sigma(\varepsilon)^{-2}$, we have $\varepsilon *_{\sigma} (T(\varepsilon^2, \varepsilon^{-2})) = \eta_1(\sigma T(1,1))$. \square

Combining this with the results of the previous subsection gives the geometric structure of the cusp end M_{Δ} . We point out one more interesting detail before summarizing the results thus far into a theorem. Recall that $T(y_1, y_2) = \mathcal{D}_C(U) \cap \mathcal{F}(y_1, y_2)$ and let

$$(17) \quad \mathcal{U}(s) := \{T(\varepsilon^r s, \varepsilon^{-r} s) \mid 0 \leq r < 2\},$$

which we will call a *(cusp section) tower* of Γ .

Proposition 3.3.3. *For each $s \in \mathbb{R}^+$, the tower $\mathcal{U}(s)$ admits a symmetry among its toroidal cross sections whereby $\forall r \in [0, 2)$, $T(\varepsilon^r s, \varepsilon^{-r} s)$ has the same number of sides as $T(\varepsilon^{2-r} s, \varepsilon^{r-2} s)$.*

Proof. Suppose $n \not\equiv_4 1$. Applying Proposition 3.2.3 to the elements $1, \sqrt{d} \in \mathbb{Z}_K$ that contribute sides to $T(s, s)$, as specified by Lemma 3.3.1, we can compute the set of lattices generated by pairs $\{z_1, z_2\} \in \mathbb{Z}_K$ that create parallelogram cross-sections in the towers $\mathcal{U}(s)$. By Lemma 3.3.2, this is $\{\varepsilon, \varepsilon\sqrt{d}\}$ at $r = 2$.

Use the same algorithm to find the integers contributing the sides of next the parallelogram below the one at $\{\varepsilon, \varepsilon\sqrt{d}\}$. We see that these are $\{\varepsilon\sigma(z_1), \varepsilon^{-1}\sigma(z_2)\}$, where $\{z_1, z_2\}$ are the integers contributing sides to the next parallelogram above the one at $s = 0$. This continues as a pairing on integers contributing parallelograms going down and up (e.g. at $s = 0$ and $s = 2$, this becomes $\varepsilon\sigma(\varepsilon) = \pm 1$ and $\varepsilon\sigma(\varepsilon\sqrt{d}) = \pm\sqrt{d}$, as expected), and applying the formula for the height given by Proposition 3.2.3 shows that this pairs $T(\varepsilon^r s, \varepsilon^{-r} s)$ to $T(\varepsilon^{-r} s, \varepsilon^r s)$. Combining this with the isometry $(\varepsilon^{-1} *_{\sigma} \eta_1)$ from $T(\varepsilon^r s, \varepsilon^{-r} s)$ to $T(\varepsilon^{r+2} s, \varepsilon^{-r+2} s)$ of Lemma 3.3.2 gives the stated pairing of $T(\varepsilon^r s, \varepsilon^{-r} s)$ and $T(\varepsilon^{2-r} s, \varepsilon^{-r+2} s)$.

When $d \equiv_4 1$, use Proposition 3.2.3 to find the next lattice $T(y_1, y_2)$ above $T(1, 1)$ and then argue the same way starting with the integers that contribute the sides to this and $T(\varepsilon^2 y_1, \varepsilon^{-2} y_2)$. \square

Table 1 shows the distribution of parallelograms in the cusp shapes for the cases up to $n = 13$, as given by applying the algorithm indicated by Proposition 3.2.3, and also exhibits the symmetry described by Proposition 3.3.3.

Let

$$(18) \quad \tilde{\mathcal{R}} := \bigsqcup_{s \in \mathbb{R}^+} \mathcal{U}(s),$$

a fundamental domain for Δ . Then, recalling that $C = \{p \in \mathcal{H}^2 \times \mathcal{H}^2 \mid N(p) \geq 1\}$ is our fundamental domain for the inversion map ι , let

$$(19) \quad \mathcal{R} := \tilde{\mathcal{R}} \cap C.$$

We summarize our results thus far in the following theorem.

Theorem 3.3.4. *The region \mathcal{R} is a fundamental domain for Γ , and $\bigsqcup_{s>1} \mathcal{U}(s)$ is homeomorphic to M_Δ . For $s > 1$, each $\mathcal{U}(s)$ is homeomorphic to the cusp section, is symmetric about an axis along which orthogonal cross sections are tori comprised of finitely many parallelograms joined by continua of hexagons, and varying s varies the $\mathcal{U}(s)$ continuously by a uniform stretching of the metric.*

□

4. VISUALIZING THE CUSP SECTION AND ITS ANOSOV DIFFEOMORPHISM

Using the notation for $\mathcal{U}(s)$ as defined by equation (17), for each $K = \mathbb{Q}(\sqrt{n})$ let

$$\mathcal{U}_n := \mathcal{U}(1).$$

Then $\mathcal{U}_n \cong T_\varphi^3$ is a canonical tower (or fundamental for the cusp section) of Γ . We now give a way to plot this in \mathbb{R}^3 allowing us to visualize the structure derived §3, in a way where its Anosov diffeomorphism is easily written down. Let

$$(20) \quad \Psi : \mathcal{H}^2 \times \mathcal{H}^2 \rightarrow \mathbb{R}^3, \quad (x_1 + y_1 i, x_2 + y_2 i) \mapsto \left(x_1, x_2, \log_\varepsilon \left(\frac{y_1}{y_2} \right) \right),$$

and let $\mathcal{C}_n := \Psi(\mathcal{U}_n)$. Then

$$\mathcal{C}_n = \left\{ (x_1, x_2, 2r) \mid (x_1, x_2) \in \pi_{\varepsilon^r, \varepsilon^{-r}}^{-1}(T(\varepsilon^r, \varepsilon^{-r})), r \in [0, 2] \right\}.$$

For any n , Proposition 3.2.3 gives an effective algorithm for computing \mathcal{C}_n given ε . We have carried this out and plotted the result for each of the the first 3 values of $n \not\equiv 4 \pmod{4}$ and $n \equiv 1 \pmod{4}$, shown in Figure 4. In the infinite tower $\Psi(\mathcal{D}_c(U))$, the tops of these towers continue to stretch exponentially above \mathcal{C}_n , and the bottoms stretch orthogonally, where translations by D along the axis of symmetry are up to identifications by U , and as dictated by Lemma 3.3.2.

Remark 4.0.1. *When $n = 5$, there is a unique parallelogram cross-section of the cusp section, whereas others have at least 2, and the complexity of the shapes quickly increases (though not uniformly) with the coefficients in the fundamental unit. Compare this with Cohn's result [5] that the classical fundamental domain has a simple floor if and only if $n = 5$, where a cusp end section is modeled using a single parallelogram.*

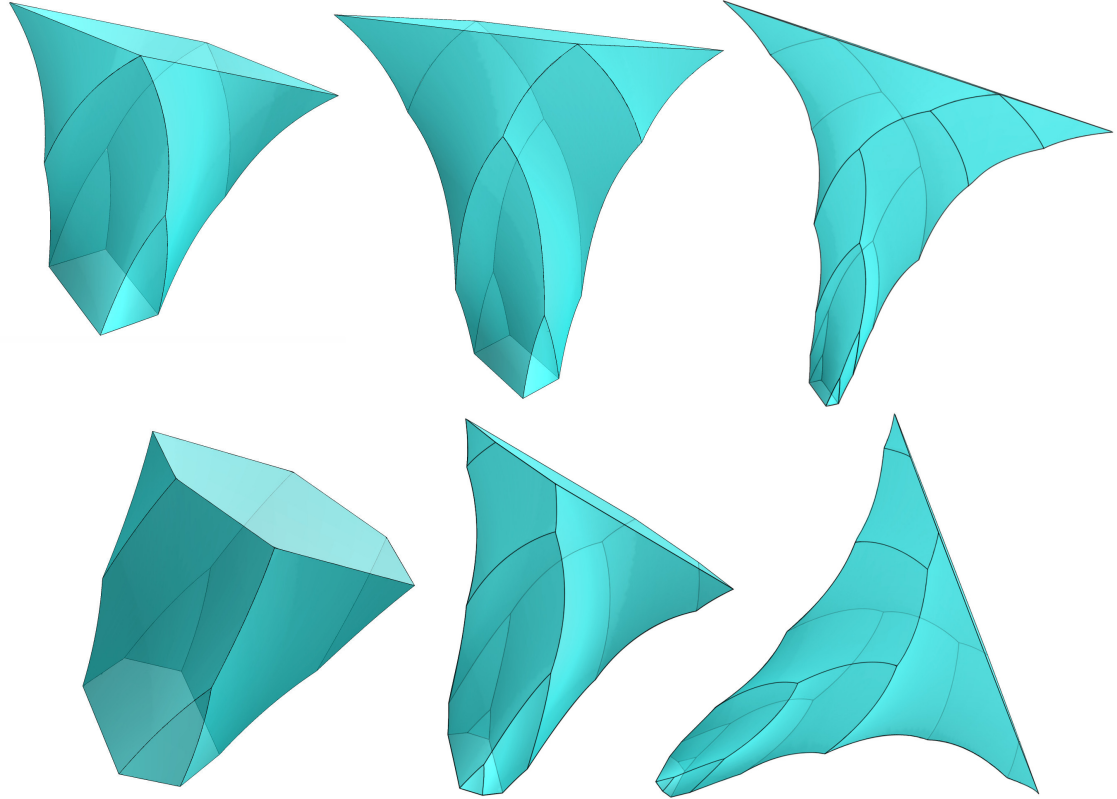


FIGURE 4. [14] Computer generated images are shown of cusp section fundamental domains \mathcal{C}_2 , \mathcal{C}_3 and \mathcal{C}_6 on the top row and of \mathcal{C}_5 , \mathcal{C}_{13} and \mathcal{C}_{17} on the bottom row, from left to right.

As a Sol 3-manifold, the Lie group structure of the cusp section is represented in \mathcal{C}_n by the multiplication rule on \mathbb{R}^3

$$(x_1, x_2, r) \bullet (x'_1, x'_2, r') := (x_1 x'_1, x_2 x'_2, r + r')$$

up to taking equivalent representatives of orbits in $\Psi(\Delta \mathcal{U}_n)$ (we will abuse notation, abbreviating this by $\Delta(\mathcal{C}_n)$). With this we can concisely write down the Anosov diffeomorphism in this model.

Theorem 4.0.2. *The map on \mathcal{C}_n defined on orbit representatives by*

$$\varphi_n : \Delta(\mathcal{C}_n) \rightarrow \Delta(\mathcal{C}_n), \quad p \mapsto (\varepsilon, \sigma(\varepsilon), 0) \bullet p$$

is an Anosov diffeomorphism of the cusp section of M_Γ .

Proof. Lemma 3.3.2 showed that $\varepsilon *_{\sigma} (T(\varepsilon^2, \varepsilon^{-2})) = \eta_1(T(1, 1))$, which extends to a diffeomorphism at each torus,

$$(\varepsilon^{-1} *_{\sigma} \circ \eta_1) : T(y_1, y_2) \rightarrow T(\varepsilon^2 y_1, \varepsilon^{-2} y_2),$$

$$(x_1 + y_1 i, x_2 + y_2 i) \mapsto (\varepsilon x_1 + \varepsilon^2 y_2 i, \varepsilon^{-1} x_1 + \varepsilon^{-2} y_2 i).$$

In $\Psi(\mathcal{D}_c(U))$, this is the Anosov diffeomorphism that attaches the bottom torus in \mathcal{C}_n to the top one, given by $(x_1, x_2, 0) \sim (\varepsilon x_1, \sigma(\varepsilon) x_2, 4)$. Under the identification of leaves given by η_1 , this descends to the map φ_n as defined above. \square

Theorem 4.0.2 implies that φ_n is an orientation-preserving or orientation-reversing map depending on the norm of ε .

We conclude this section with a brief comment about compactification. As the height $y_1 y_2$ increases, the metric contracts uniformly along the x_1 and x_2 axes in \mathcal{C}_n , but remains constant along the vertical axis, since we always have $\frac{\varepsilon^r s}{\varepsilon^{-r} s} = \varepsilon^{2r} \in [1, \varepsilon^4]$. Thus the cusp end is approaching a circle on $\partial(\mathcal{H}^2 \times \mathcal{H}^2)$ where the variation in toroidal cross-sections becomes irrelevant, implying a geometric compactification of M_{Δ} by a circle.

5. SIMPLE FLOORS

Our ability to create simple floors comes from the fact that we have modeled the cusp section as a 3-dimensional tower where R_U deforms as the level varies. The floor can then be seen as the 3-dimensional region that intersects $\mathcal{U}(s)$ as a continuum of surfaces as we change s . This follows easily from the construction.

Theorem 5.0.1. *The boundary of \mathcal{R} has finite volume if and only if $K = \mathbb{Q}(n)$ with $n = 2, 3, 5$ or 13 .*

Proof. Denote the complement of C by \overline{C} and let

$$(21) \quad B := \{(x_1, x_2) \in \mathbb{R}^2 \mid |x_1 x_2| \leq 1\},$$

the region in \mathbb{R}^2 bounded away from $(0, 0)$ by the 4 hyperbolas where $|x_1 x_2| = 1$. As $s \rightarrow 0$, the set $\pi_{y_1 s, y_2 s}(\overline{C} \cap \mathcal{F}_H(y_1 s, y_2 s))$ approaches B . If we can find some $s \in \mathbb{R}^+$ such that the point $p \in \pi_{y_1 s, y_2 s}(T(\pi_{y_1 s, y_2 s}))$ lies in B , then we are guaranteed some $s' > s$ where $p \in \pi_{y_1 s', y_2 s'}(T(\pi_{y_1 s', y_2 s'}) \cap \partial C)$, i.e. $p + (y_1 s' i, y_2 s' i) \in T(\pi_{y_1 s', y_2 s'}) \cap \partial C$. Conversely, a point $p \in \pi_{y_1 s, y_2 s}(T(y_1 s, y_2 s)) \setminus B$ will not be on ∂C for any choice of s .

We rule out other values of n by noticing that for those, simplicity fails already at $T(1, 1)$. By Lemma 3.3.1, $T(1, 1)$ is bounded by the mediatrixes $m(\tau_z)$ over

$$z = \begin{cases} \pm 1, \pm \sqrt{d} & ; \quad n \not\equiv_4 1 \\ \pm 1, \pm \frac{1+\sqrt{d}}{2}, \pm \frac{1-\sqrt{d}}{2} & ; \quad n \equiv_4 1 \end{cases}.$$

Since each $m(\tau_z) \cap \mathcal{F}(1, 1)$ is the Euclidean perpendicular bisector of the points $(0, 0)$ and $(z, \sigma(z))$, we need only compute when $T(1, 1)$ contains one of the points $(1, \pm 1) \in \partial B$. Since $m(\tau_1)$ passes through the point $(\frac{1}{2}, -\frac{1}{2})$, we need only consider the point $(1, -1)$.

When $d \not\equiv_4 1$, $(1, -1) \notin \pi_{1,1}(T(1, 1))$ if and only if it is farther from $(0, 0)$ than the point $\left(\frac{\sqrt{n}}{2}, -\frac{\sqrt{n}}{2}\right) \in m(\tau_{\sqrt{d}})$, which happens if and only if $n = 2$ or 3 . When $d \equiv_4 1$, $(1, -1) \notin \pi_{t,t}(T(t, t))$ if and only if it is further from $(0, 0)$ than the point $\left(\frac{\sqrt{n}}{4}, -\frac{\sqrt{n}}{4}\right) = m\left(\tau_{\frac{1+\sqrt{d}}{2}}\right) \cap m\left(\tau_{\frac{1-\sqrt{d}}{2}}\right)$, which happens if and only if $n = 5$ or 13 .

Applying Proposition 3.2.3 for the values of n stated in the theorem and checking that the towers (this data is listed in Table 1) remain inside the region B finishes the proof. \square

Corollary 5.0.2. *When $n = 2, 3, 5$ or 13 , \mathcal{R} admits a thick-thin decomposition into a cusp end homeomorphic to $\tilde{\mathcal{R}}$, and a compact region $\bigsqcup_{0 < s \leq 1} \mathcal{U}(s) \cap C$.*

For fundamental domains of this nature, $F(\mathcal{R}) = \mathcal{R} \cap \partial C$, which is a 3-dimensional region bijectively homeomorphic to a cusp section, showing up as 2-dimensional cross sections of towers as we vary s in $\mathcal{U}(s)$. In these cases, we can start with the tower $\mathcal{U}(1)$, where $\forall p = (x_1 + \varepsilon^r s i, x_2 + \varepsilon^{-r} s i) \in \mathcal{U}(s)$, $N(p) > 1$, then for each such p , there exists a unique $s < 1$ such that the point

$$p_s := (x_1 + \varepsilon^r s i, x_2 + \varepsilon^{-r} s i) \in \mathcal{U}(s')$$

satisfies $N(p_s) = 1$. In this case $F(\tilde{\mathcal{R}}) = \bigcup_{p \in \mathcal{U}(s)} \{p_s\}$. As s decreases from some sufficiently large value, portions of a cusp section are omitted as parts of it enter \overline{C} , exemplified in Figure 5.

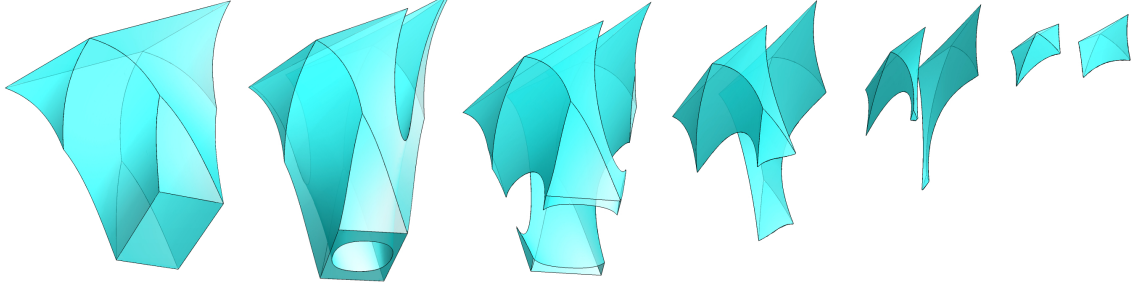


FIGURE 5. [14] The remaining portion of a cusp section lying above an affine-simple floor in cusp sections $\mathcal{U}(s)$ is shown as the height decreases, from left to right, in the case $n = 2$ (under the map Ψ). The boundary surface(s) interior to a section $\mathcal{U}(s)$ is the part of the floor intersecting that tower, which deforms continuously as s decreases. Here we see the region separating into 2 pieces which then degenerate into a pair of upper corners (which eventually vanish).

When $\partial\mathcal{R}$ does not have finite volume, portions of $\mathcal{U}(s) \cap C$ will persist regardless of how small s becomes, but occur in connected components identified under the toroidal face

pairings (exemplified in Figure 6). Appealing to Definition 2.3.1, the following proposition shows that these remaining portions of the towers, up to varying the height, still represent points in ∂M_Γ up to the action of U .

Proposition 5.0.3. *\mathcal{R} has an affine-simple floor for all n .*

Proof. We need to show that for all $p \in T(y_1, y_2)$, there exists some $z \in \mathbb{Z}_K$ and some $s \in \mathbb{R}^+$ such that $\tau_z(p) \in \partial C \cap \mathcal{F}(sy_1, sy_2)$. As in the proof of Theorem 5.0.1, it suffices to look at the points in an arbitrary tower $\mathcal{U}(s)$ where cross-sections (under the appropriate maps π_{y_1, y_2}) do not lie in the region B .

The sides of $T(y_1, y_2)$ consist of pairs whose lengths are not commensurable (not equivalent up to multiplication in \mathbb{Q}), thus the coordinate axes densely fill $\pi_{y_1, y_2}(T(y_1, y_2))$ under the quotient by U . Since B contains an open neighborhood of the coordinate axes, it fills $T(y_1, y_2)$ under this quotient, guaranteeing the existence of some $z \in \mathbb{Z}_K$ so that $\pi_{y_1, y_2}(\tau_z(p)) \in (\pi_{y_1, y_2}\mathcal{F}(y_1, y_2)) \cap B$. So as in the proof of Theorem 5.0.1, we can raise the height via some $s' \in \mathbb{R}^+$, giving $\pi_{y_1 s', y_2 s'}(\tau_z(p)) \in (\pi_{y_1 s', y_2 s'}\mathcal{F}(y_1 s', y_2 s')) \cap \partial C$. \square

This means that the cusp section is homeomorphic to the boundary, up to some connected region(s) where we choose alternative representatives of the orbit of U . Also, any such regions occur symmetrically about $\mathbb{R}^+i \times \mathbb{R}^+i$, and identify in pairs via the toroidal face pairings on the sides of each tower and the Anosov diffeomorphism connecting the bottom of each tower to the top. Figure 6 shows an example of a set of points collected by their location in their respective tower, that contribute to the portion of $\partial \mathcal{R}$ of finite volume, in the case when $\partial \mathcal{R}$ is not contained in ∂C .

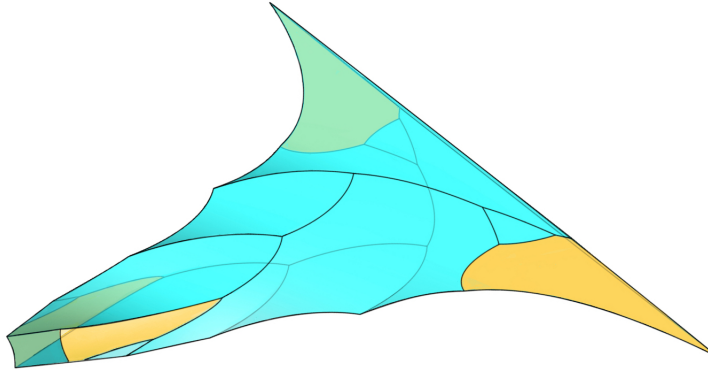


FIGURE 6. [14] The finite volume portion of the boundary is shown for the case $n = 6$, as the points in $\mathcal{R} \cap \partial C$ that appear in some tower up to varying the height. Surfaces exposed by removing the non-finite-volume portion are colored orange. Compare to the image in Figure 4 of the full cusp section tower for $n = 6$.

6. ACKNOWLEDGEMENTS

This research paper has been made possible thanks to the financial support generously given by the FORDECyT-CONACyT (Mexico) grant #265667, Universidad Nacional Autónoma de México. The second author was financed by grant IN106817, PAPIIT, DGAPA, Universidad Nacional Autónoma de México. The authors also express their gratitude to Ian Agol, Jesse Ira Deutsch, Ben McReynolds and Jorge Millan for helpful suggestions and discussion, and to Dennis Ryan and Simon Woods for help with creating the computer generated images.

REFERENCES

- [1] Wolf Barth, Klaus Hulek, Chris Peters, and Antonius Van de Ven. *Compact complex surfaces*, volume 4. Springer, 2015.
- [2] Otto Blumenthal. Über modulfunktionen von mehreren veränderlichen (Erste Hälfte). *Mathematische Annalen*, 56:509–548, 1903.
- [3] Otto Blumenthal. Über modulfunktionen von mehreren veränderlichen (Zweite Hälfte). *Mathematische Annalen*, 58:497–527, 1904.
- [4] Desmos Graphing Calculator. 2017. available at <https://www.desmos.com/calculator>.
- [5] Harvey Cohn. A numerical survey of the floors of various Hilbert fundamental domains. *Mathematics of Computation*, 19(92):594–605, 1965.
- [6] Harvey Cohn. On the shape of the fundamental domain of the Hilbert modular group. In *Proc. Symp. Pure Math*, volume 8, pages 190–202, 1965.
- [7] Harvey Cohn. Note on how Hilbert modular domains become increasingly complicated. *Journal of Mathematical Analysis and Applications*, 15(1):55–59, 1966.
- [8] Harvey Cohn. Some computer-assisted topological models of Hilbert fundamental domains. *Mathematics of Computation*, 23(107):475–487, 1969.
- [9] Jesse Deutsch. A computational approach to Hilbert modular group fixed points. *Mathematics of computation*, 71(239):1271–1280, 2002.
- [10] Jesse Ira Deutsch. Conjectures on the fundamental domain of the Hilbert modular group. *Computers & mathematics with applications*, 59(2):700–705, 2010.
- [11] Peter Engel. Dirichlet domains. In *Geometric Crystallography*, pages 13–21. Springer, 1986.
- [12] Fritz Götzky. Über eine zahlentheoretische anwendung von modulfunktionen zweier veränderlicher. *Mathematische Annalen*, 100(1):411–437, 1928.
- [13] Friedrich Hirzebruch. The Hilbert modular group, resolution of the singularities at the cusps and related problems. In *Séminaire Bourbaki vol. 1970/71 Exposés 382–399*, pages 275–288. Springer, 1971.
- [14] Wolfram Research, Inc. Mathematica, Version 11.1.10. Champaign, IL, 2017.
- [15] Hans Maass. *Über Gruppen von hyperabelschen Transformationen*. Weiss, 1940.
- [16] Curtis T McMullen. Foliations of Hilbert modular surfaces. *American Journal of Mathematics*, pages 183–215, 2007.
- [17] David Ben McReynolds. Cusps of arithmetic orbifolds. *arXiv preprint math/0606571*, 2006.
- [18] David Ben McReynolds. Cusps of Hilbert modular varieties. In *Mathematical Proceedings of the Cambridge Philosophical Society*, volume 144, pages 749–759. Cambridge Univ Press, 2008.
- [19] Carl Ludwig Siegel. On advanced analytic number theory. *Tata Institute for Fundamental Research, Bombay*, 1961.
- [20] Gerard Van Der Geer. *Hilbert modular surfaces*, volume 16. Springer Science & Business Media, 2012.

TABLE 1. Parallelograms occurring in the cusp section towers, for the first 7 values of n , are indicated by their levels and the integers contributing their sides. The examples are specified by giving their fundamental unit ε , and when possible, other entries are written in the form ε^n , $n \in \mathbb{N}$.

ε	level	sides
$1 + \sqrt{2}$	1	$1, \sqrt{2}$
	ε^2	$1, \varepsilon$
	ε^4	$\varepsilon, \varepsilon\sqrt{2}$
$2 + \sqrt{3}$	1	$1, \sqrt{3}$
	ε	$1, 1 + \sqrt{3}$
	ε^3	$1 + \sqrt{3}, \varepsilon$
	ε^4	$\varepsilon, \varepsilon\sqrt{3}$
$\frac{1+\sqrt{5}}{2}$	ε^2	$1, \varepsilon$
$5 + 2\sqrt{6}$	1	$1, \sqrt{6}$
	$\frac{1}{5}(7 + 2\sqrt{6})$	$1, 1 + \sqrt{6}$
	ε	$1, 2 + \sqrt{6}$
	ε^2	$2 + \sqrt{6}, 3 + \sqrt{6}$
	ε^3	$2 + \sqrt{6}, \varepsilon$
	$\frac{1}{5}(10,087 + 4,118\sqrt{6})$	$\varepsilon, 7 + 3\sqrt{6}$
	ε^4	$\varepsilon, \varepsilon\sqrt{6}$
$8 + 3\sqrt{7}$	1	$1, \sqrt{7}$
	$\frac{1}{3}(4 + \sqrt{7})$	$1, 1 + \sqrt{7}$
	$\frac{1}{3}(11 + 4\sqrt{7})$	$1, 2 + \sqrt{7}$
	$\frac{1}{3}(172 + 65\sqrt{7})$	$2 + \sqrt{7}, 3 + \sqrt{7}$
	$\frac{1}{3}(884 + 319\sqrt{7})$	$3 + \sqrt{7}, 5 + 2\sqrt{7}$
	$\frac{1}{3}(13,451 + 5,084\sqrt{7})$	$5 + 2\sqrt{7}, 8 + 3\sqrt{7}$
	$\frac{1}{3}(43,684 + 16,511\sqrt{7})$	$\varepsilon, 13 + 5\sqrt{7}$
	ε^4	$\varepsilon, \varepsilon\sqrt{7}$
$10 + 3\sqrt{11}$	1	$1, \sqrt{11}$
	$\frac{1}{5}(6 + \sqrt{11})$	$1, 1 + \sqrt{11}$
	$\frac{1}{7}(15 + 4\sqrt{11})$	$1, 2 + \sqrt{11}$
	ε	$1, 3 + \sqrt{11}$
	$\frac{1}{5}(1,854 + 559\sqrt{11})$	$3 + \sqrt{11}, 7 + 2\sqrt{11}$
	ε^3	$3 + \sqrt{11}, \varepsilon$
	$\frac{1}{7}(137,295 + 41,396\sqrt{11})$	$\varepsilon, 13 + 4\sqrt{11}$
	$\frac{1}{5}(212,526 + 64,079\sqrt{11})$	$\varepsilon, 23 + 7\sqrt{11}$
	ε^4	$\varepsilon, \varepsilon\sqrt{11}$
$\frac{3+\sqrt{13}}{2}$	$\frac{1}{6}(7 + \sqrt{13})$	$1, \frac{1+\sqrt{13}}{2}$
	ε^2	$1, \varepsilon$
	$\frac{1}{3}(101 + 28\sqrt{13})$	$\varepsilon, \frac{5+\sqrt{13}}{2}$